CIRP Annals - Manufacturing Technology 74 (2025) 399–403

Contents lists available at ScienceDirect

CIRP Annals - Manufacturing Technology

journal homepage: https://www.editorialmanager.com/CIRP/default.aspx

Advanced double-flush riveting for multistage forming tools

Carlos M.A. Silva[a], João P.M. Pragana[a], Rui F.V. Sampaio[a], Ivo M.F. Bragança[b], Paulo A.F. Martins (1)[a,*]

[a] IDMEC, Instituto Superior Tecnico, Universidade de Lisboa, 1049-001 Lisbon, Portugal
[b] CIMOSM, Instituto Superior de Engenharia de Lisboa, Instituto Politécnico de Lisboa, 1959-007 Lisbon, Portugal

ARTICLE INFO

Article history:
Available online 23 April 2025

Keywords:
Cold forming
Joining
Multistage tools

ABSTRACT

This paper presents a novel double-flush riveting process for creating lap joints in sheet metal parts. The process involves punching, forging, and shaving to produce countersunk holes with precise geometry, followed by compression of cylindrical rivets into the holes of two overlapped sheet parts to create form-closed mechanical interlocks. Experimental and numerical analyses examine the influence of the primary process parameters on interlock quality and required forming and destructive forces. The investigation is a step forward in joining technology by offering a simple alternative to welding, bonding, and mechanical joining, with seamless integration into multistage forming tools.

1. Introduction

Welding, bonding, and mechanical joining are the leading joining technologies used to assemble multi-module and multi-material sheet parts. Each technology has well-known advantages and limitations, which have been comprehensively discussed in several state-of-the-art reviews (e.g., [1]). One issue, often overlooked in literature but of paramount industrial significance, is the integration of these joining technologies into multistage forming presses [2]. This is a complex task but assembling different modules into one sheet part or reinforcing them locally while avoiding post-multistage operations is very important for many industries, such as automotive. The question that naturally arises is: Can processes built upon welding, bonding, and mechanical joining technologies be seamlessly integrated into multistage (progressive or transfer) forming tools, or do they need to be performed using other machines and accessories afterward?

In general, welding and bonding processes cannot be integrated because they require the usage of specialized equipment (e.g., welding machines, adhesive application guns, or rollers) and accessories like clamps, jigs, and fixtures to hold the sheet parts steady during the heat-cooling cycles of welding and to apply pressure during the curing time of the adhesives [3].

Mechanical joining with fasteners is also challenging to integrate into multistage forming tools. Alternative mechanical joining processes commonly known as joining by plastic deformation processes [4], like self-pierce riveting, for example, require complicated adaptation of available systems to specific multistage tool production conditions. They are also limited by the total thickness of the joints (between 1.6 and 8 mm), the need to position thinner and softer sheets on the punch side, and the creation of protrusions above and below the sheet surfaces [5].

Clinching, while easier to integrate, creates joints with lower strength [6] due to a weaker interlock mechanism than self-pierced joints, which benefit from the rivet spreading in the lower sheet to create a more secure and consistent joint. Material protrusions on one side of the joint may also pose challenges in multistage forming tools, further complicating the integration [7].

The integration challenges and limitations mentioned above underscore the need for further research and development in this area. This paper aims to address this topic by presenting an advanced double-flush riveting joining by plastic deformation process tailored to multistage forming tool systems. The process is built upon a previous double-flush riveting (DFR) process, which involves punching the sheet parts to be joined and compressing solid rivets into the punched holes to create lap joints with flat surfaces on both sides of the sheet parts [8] (Fig. 1a). However, the new process to be presented in this paper takes a significant step further by setting up a reliable and repeatable fabrication sequence specifically designed for industrial use in multistage forming tools (Fig. 1b), ensuring its practicality and applicability.

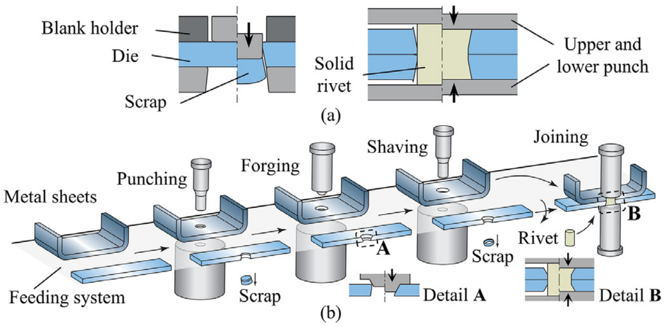

Fig. 1. Schematic representation of the (a) double-flush riveting (DFR) and (b) new proposed advanced double-flush riveting (ADFR) processes for the assembly of sheet metal parts.

* Corresponding author.
E-mail address: pmartins@tecnico.ulisboa.pt (P.A.F. Martins).

https://doi.org/10.1016/j.cirp.2025.03.040

The new proposed double-flush riveting process, hereafter named "advanced double-flush riveting" (ADFR), is designed to solve two significant concerns about the previous DFR process that were raised by industrial partners of the Hi-REV consortium [9]: (i) the inconsistent morphology of the cut surfaces resulting from punch wear during production, and (ii) the limited maximum angle of the tapered cut surface (also known as the "breakout angle"), which is generally below 15 degrees, limiting the formation of reliable, form-closed joints.

The overall strategy of the ADFR process includes additional forging and shaving operations to achieve a more inclined and high-quality countersunk hole (Fig. 1b). This paper details the numerical and experimental development of the ADFR process, presenting results for the connection of high-strength steel parts. It also comprehensively compares results in shear and peel destructive tests against alternative resistance spot welded (RSW) joints, ensuring a thorough perspective of the ADFR process.

2. Materials and methods

2.1. Materials and flow curves

The ADFR process was validated by fabricating unit cells representing lap joints with geometries suitable for destructive shear and peel tests. Each unit cell was constructed using 2 mm thickness sheets of S500MC (WN. 1.0984, DIN EN 10,149–2) hot-rolled, high-strength, low-alloy steel and solid cylindrical rivets machined from S235JR (WN. 1.0038, DIN EN 10,025–2) structural steel rods with 6 mm diameter. The latter were machined from the as-supplied rods and from rods previously annealed at 700 °C for approximately one hour.

The flow curve of the S500MC sheet material was derived from tensile tests on specimens cut at 0°, 45°, and 90° relative to the rolling direction and from stack compression tests. The tensile test results revealed that anisotropy could be neglected, and the stack compression tests helped determine the strain-hardening response at higher strain values, similar to those encountered in the fabrication of the joints. Fig. 2 shows the experimental flow curve, which integrates tensile and stack compression test results.

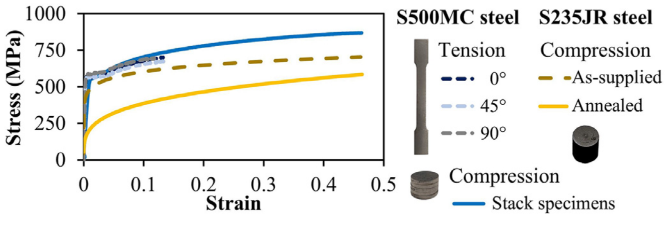

Fig. 2. Experimental flow curves of the S500MC sheet and S235JR (as-supplied and annealed) rod materials at ambient temperature.

The flow curves of the S235JR structural steel rod in the as-supplied and annealed conditions were determined from compression tests with cylindrical specimens, and the results are also shown in Fig. 2.

2.2. Advanced double-flush riveting

The DFR process involves punching the sheet parts to be joined and pressing solid cylindrical rivets into the punched holes to create lap joints with flat surfaces on both sides (Fig. 1a). A key distinction of the novel ADFR process is the introduction of two additional intermediate operations - forging and shaving - which are critical for controlling the quality and geometry of the countersunk holes and removing any burrs or excess material resulting from previous punching and forging. This is crucial to ensure a smooth insertion of the rivets for the final operation in which the sheets are mechanically interlocked.

The tool depicted in Fig. 3 was designed to replicate the punching, forging, and shaving multistage operations in a laboratory environment using unit cells. It includes an extra operation to bend the sheets to create specimens for peel tests, which evaluate the strength of the joints fabricated by ADFR.

The tool comprises two flat, precision-ground metal plates (the upper and lower bolsters), which serve as the mounting surfaces for all the remaining components and for its installation in the Instron SATEC 1200 kN hydraulic testing machine. Four pillars and guide bushes,

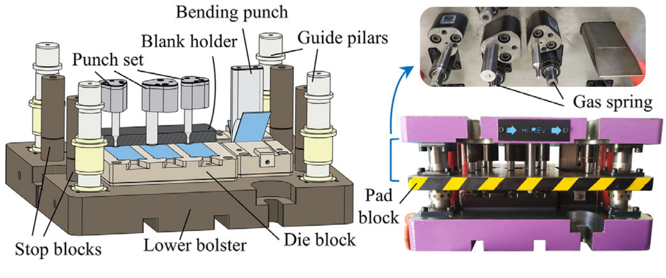

Fig. 3. The laboratory tool system used to replicate the punching, forging and shaving operations of the novel ADFR process. The last station of the tool is used to create 90° bent specimens for destructive peel tests.

which ensure accurate alignment and smooth movement of the punches relative to their dies, help maintain the precision and repeatability of the punching, forging, and shaving operations.

An intermediate ground plate (pad block), which is guided on the pillars through ball-bearing bushes, serves as a blank holder to hold the unit cells in position under a maximum compression force of 45 kN imposed through ten small gas springs distributed across the plate's surface. Quick-change punch retainers are included for easy replacement of the punches used in the three operations mentioned above. This feature ensures the tool is easily adjustable for different geometries of the countersunk holes.

The final operation of the novel ADFR process, which consists of pressing the solid cylindrical rivets into the countersunk holes to create form-closed lap joints, was carried out with another tool retrieved from the experiments with the previous DFR process [8].

2.3. Work plan

Table 1 presents the geometry of the unit cells used in the lap shear and peel destructive tests, along with the main process parameters for both the ADFR and RSW processes. The RSW was included for comparison purposes, and its parameters were chosen to create welding nuggets with diameters comparable to those of the ADFR joints. The initial height of the solid cylindrical rivets used in the ADFR joints was determined so that the rivets would match the volume of the countersunk holes after shaving.

Table 1
Main process parameters used in the ADFR and RSW processes.

Unit Cell	
Length l (mm)	150
Width w (mm)	50
Overlapped length l_o (mm)	50
Thickness t (mm)	2
Rivet diameter d_r (mm)	5
Advanced double-flush riveting (ADFR)	
Punching diameter d_p (mm)	5.1
Forging angle α (degree)	20, 30
Forging depth d (mm)	1.6
Shaving diameter d_s (mm)	5
Resistance spot welding (RSW)	
Current (kA)	6
Force (kN)	1.5
Time (s)	0.2
Electrode diameter d_e (mm)	8

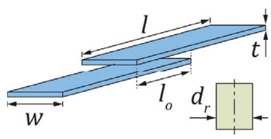

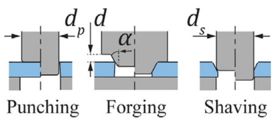

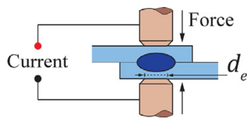

2.4. Numerical modelling

Plastic deformation plays a critical role in material separation during punching and shaving operations. However, the changes in stress and strain distributions resulting from these operations are confined to material located very close to the shearing zones. Therefore, the numerical simulation of the ADFR fabrication sequence using the in-house finite element software I-FORM [10] was focused on the forging operation that shapes the countersunk holes from previously punched holes, and on the final operation where the solid rivets are compressed into the countersunk holes (previously calibrated by shaving) to create the required form-closed lap joints.

The numerical simulation emphasizes the practical implications of the countersunk hole geometry, particularly the inclination of the tapered surface and the material strain-hardening resulting from the forging operation into the final operation of the ADFR sequence, where the overlapped sheets are mechanically interlocked. This understanding is crucial for optimizing the design and fabrication of the joints.

The sheets and rivets were modeled as deformable objects following the Levy-Mises constitutive equations, and plastic deformation in the neighborhood of the joints was assumed to be rotationally symmetric. The punches and dies were modeled as rigid contact-friction objects. Friction is modeled by means of the law of constant friction with a factor $m = 0.1$, after validating the finite element predictions of force evolution and the geometry of the joint cross-sections against actual values and shapes. The CPU time for a typical model with 4000 elements undertaking the simulation of the forging and compression operations was below 15 min in a computer equipped with an Intel Core i7 - 6950X processor.

3. Results and discussion

3.1. Forging operation

The forging operation (Fig. 4a) induces plastic deformation in the material near the previously punched holes to shape countersunk holes with controlled surface quality and inclination angle α of the tapered surface. The strain hardening resulting from forging is crucial in enhancing the final riveting operation. It strengthens the sheet material, which acts as a tool in the hole's vicinity, allowing the solid rivets to be later compressed into the countersunk holes of the overlapped sheets to create sound form-closed lap joints.

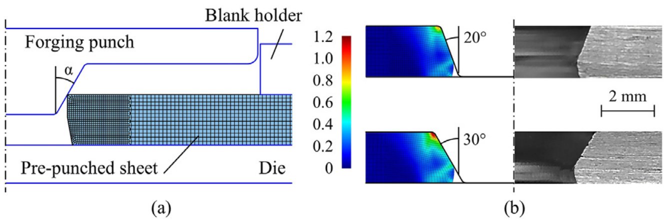

Fig. 4. (a) Detail of the finite element model of the forging operation and (b) effective strain distribution with pictures of the cross-section of the countersunk holes for two different inclination angles α.

Strain hardening increases with the inclination angle α (Fig. 4b), but larger angles than those shown in these figures can lead to excessive radial movement of the material, making it challenging to achieve the required hole diameter.

The inclusion of the forging operation to shape the countersunk holes is responsible for ADFR's standing out from alternative solutions built upon machining. The forging operation not only shapes the countersunk holes but also helps integrate ADFR effectively into multistage forming tools, showcasing its adaptability and versatility.

3.2. Riveting operation

After shaving the countersunk holes of the two overlapped sheets to remove any burrs or excess material that prevent rivets from being correctly placed in position inside the holes, the rivets are forced into the countersunk holes by compression to create form-closed lap joints without material protrusions above or below the sheet surfaces (Fig. 5).

As the inclination angle α increases, the initial height of the rivet required to ensure complete filling of the countersunk hole also needs to be increased. This results in higher effective strain values at both the upper and lower edges of the plastically deformed rivets. Consequently, there is greater radial displacement of the sheets, which, at an inclination angle $\alpha = 45^\circ$, leads to shortages of rivet material (see Fig. 6a) and undesirable bending of the sheets. This occurs even though high contact interfacial pressures are achieved after unloading.

These results emphasize the importance of limiting inclination angles to 30° (see Fig. 5b).

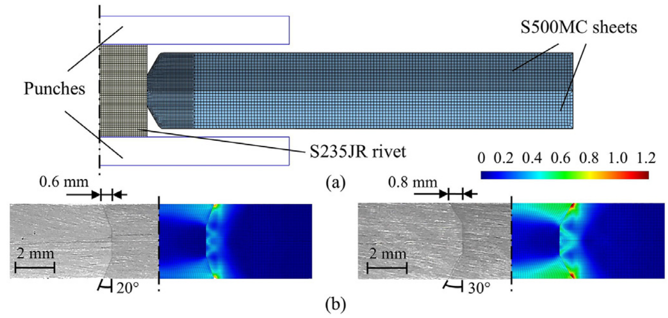

Fig. 5. (a) Finite element model for the final riveting operation to obtain a form-closed lap joint and (b) effective strain distribution with pictures of the cross-section of the joints for two different inclination angles α.

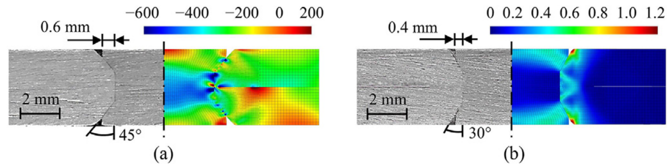

Fig. 6. (a) Radial stress after unloading using annealed rivets and a countersunk hole with $\alpha = 45^\circ$ and (b) effective strain at the end of loading using as-supplied rivets and a countersunk hole with $\alpha = 30^\circ$. The pictures show the corresponding cross-section of the joints.

The advantage of annealing the rivets is clear by comparing the interlocking distance i in Fig. 5b (right) with that in Fig. 6b (right), where the rivets were used in the as-supplied condition (i.e., without being annealed).

As observed, as-supplied rivets, which possess higher strength than the annealed ones and closer to the sheet strength, cause more significant deformation of the inner diameter of the countersunk hole. In contrast, annealed rivets effectively prevent such deformation, resulting in a larger interlocking distance i and a form-closed lap joint that will withstand greater destructive forces, as demonstrated in the following section of the paper.

In conclusion, it is paramount to use rivets with a lower stress-strain response than that of the sheets. This prevents the sheets from experiencing significant deformation, allowing them to act as dies and effectively providing better mechanical interlocks.

3.3. Forces

Two types of force-displacement evolution are of interest to the project and design of the new ADFR joints. The first type, plot with different colors in Fig. 7, shows the evolutions of the punching (P), forging (F), shaving (S), and riveting (R) forces corresponding to these individual operations during a press stroke.

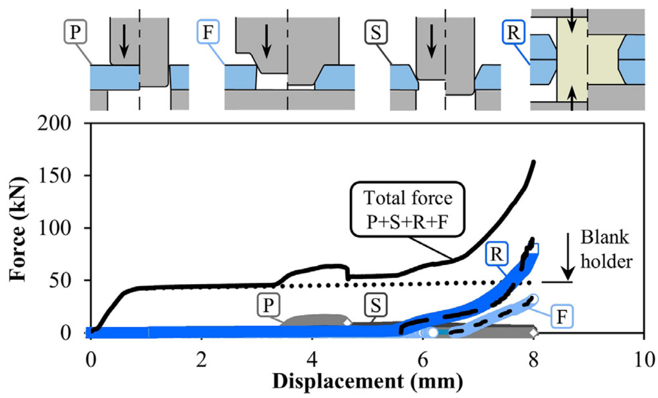

Fig. 7. Experimental force vs. displacement evolutions for the shearing, forging, shaving and final riveting operations. Finite element estimates are enclosed as dashed lines for the operations that were numerically simulated. Note: results were obtained for annealed rivets and countersunk holes with $\alpha = 30^\circ$.

The first three evolutions (P, F and S) were acquired from the tool system shown in Fig. 3, while the riveting (R) force evolution to create the form-closed joints was obtained using another tool available from the previous DFR process, as mentioned earlier. The start of riveting force evolution in Fig. 7 ensures compatibility with the forging operation at the end of the press stroke. The summation of the evolution trend of each operation plus the blank holder force is plotted as a black solid line, indicating the total force required by the ADFR process to fabricate the specific joints of this investigation in a multistage forming tool.

The agreement with the finite element predictions for the forging and final riveting operations (refer to the dashed lines) is very good and justifies the decision to exclude the punching and shaving operations from numerical simulation due to their very localized impact on neighboring material deformation.

The second type of force-displacement evolution, shown in Fig. 8, is derived from the shear and peel destructive tests of the ADFR joints, performed in accordance with the standards for the mechanical testing of blind riveted joints at ambient temperature [11]. The tests are depicted in the corresponding plot and were conducted until failure using a universal testing machine. A minimum of three tests were carried out for each joint type. As seen, the maximum forces that the joints can safely withstand before failure in the two types of tests increase with the inclination angle α because of the rise in the interlocking distance *i*, like in the case of self-pierce riveting [12].

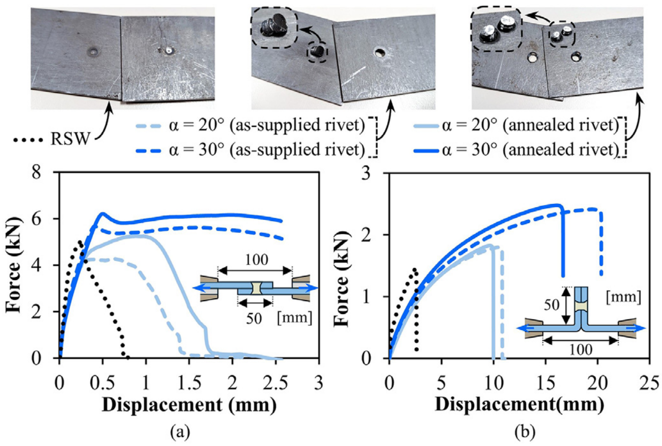

Fig. 8. Experimental force vs. displacement evolutions for the (a) shear and (b) peel destructive tests performed on joints fabricated by ADFR and RSW.

Results for the inclination angle $\alpha = 30^{\circ}$ also show that the joints fabricated with annealed rivets performed better than those with as-supplied rivets. The reason for this is shown in the pictures of the destructive peel joints enclosed in Fig. 8, showing that the joints with annealed rivets fail by shearing while those with as-supplied rivets fail by disengagement after some bending.

Fig. 8 also shows the destructive forces compared to those obtained for joints fabricated by RSW. The better performance of the form-closed joints underscores the potential of integrating the innovative ADFR process into multistage forming tools to reduce the number of RSW joints, particularly in the automotive industry.

3.4. Industrial application

This final section of the paper presents a practical application of the proposed technology, focusing on the assembly of the front driver's side reinforcement of the body-in-white structure of an automotive van. As shown in Fig. 9, this industrial application demonstrates the feasibility of the ADFR process in fabricating the part by joining a zinc-coated E275D carbon steel stamped sheet with a DP590 dual-phase steel structural reinforcement, which have different and thinner thicknesses than those used in the unit cell configurations discussed previously.

As illustrated by details A and B of Fig. 9, achieving tight lap contact was possible throughout the assembly, even in areas somewhat distant from where the rivets were applied. This resulted in joints that were free from protrusions or shortages of riveting material and

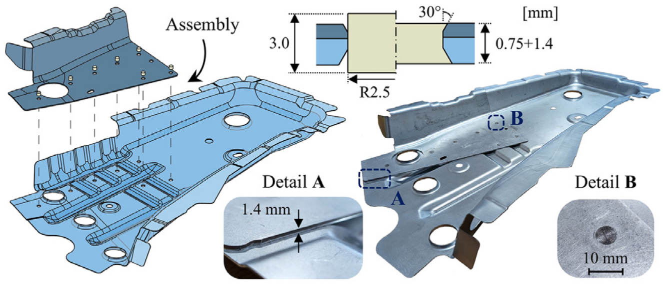

Fig. 9. The innovative ADFR process for assembling the front driver's side reinforcement of a van, highlighting (A) complete lap tightness and (B) no material protrusions or shortages at the joints.

demonstrated the potential of the ADFR process as a reliable alternative to conventional RSW for assembling complex parts.

4. Conclusions

The novel advanced double-flush riveting (ADFR) process involves a series of operations that can be seamlessly integrated into multistage forming tools. Unlike earlier variants that only used punching and riveting, this process adds forging and shaving to ensure the countersunk holes have the correct geometry under repeatable and reliable conditions. Countersunk holes with tapered surface angles $\alpha > 30^{\circ}$, are not recommended, as they cause significant radial displacement, leading to rivet material shortages and undesirable sheet bending.

The solid cylindrical rivets are easy to manufacture, and their suitable ductility minimizes the risk of formability issues such as buckling or cracking. These rivets are designed to have a lower strength than the sheets they join, which helps prevent unwanted deformation and ensures the formation of strong mechanical interlocks. Furthermore, the final joints do not impose any design limitations regarding material positioning or protrusions. This flexibility, combined with improved mechanical performance compared to resistance spot welding, makes ADFR a straightforward yet effective alternative to welding, bonding, and other mechanical joining methods.

Declaration of interests

The authors declare that they have no known competing financial interests or personal relationships that could have appeared to influence the work reported in this paper. The author is an Editorial Board Member/Editor-in-Chief/Associate Editor/Guest Editor for *[Journal name]* and was not involved in the editorial review or the decision to publish this article.

CRediT authorship contribution statement

Carlos M.A. Silva: Writing – review & editing, Visualization, Validation, Resources, Methodology, Investigation, Funding acquisition, Data curation, Conceptualization. **João P.M. Pragana:** Writing – review & editing, Visualization, Validation, Software, Resources, Methodology, Investigation, Data curation, Conceptualization. **Rui F.V. Sampaio:** Writing – review & editing, Validation, Software, Resources, Methodology, Investigation, Data curation, Conceptualization. **Ivo M.F. Bragança:** Writing – review & editing, Validation, Resources, Methodology, Investigation, Data curation, Conceptualization. **Paulo A.F. Martins:** Writing – review & editing, Writing – original draft, Supervision, Resources, Methodology, Funding acquisition, Conceptualization.

Acknowledgments

The authors would like to acknowledge the support provided by Fundação para a Ciência e a Tecnologia (FCT) and IDMEC for its financial support via the project LAETA Base Funding (DOI: 10.54499/UIDB/50022/2020) and PRR R2UTechnologies. The financial support of MCG – Mind for Metal is also acknowledged.

References

[1] Chastel Y, Passemard L (2014) Joining technologies for future automobile multi-material modules. *Procedia Engineering* 81:2104–2110.
[2] Meschut G, Janzen V, Olfermann T (2014) Innovative and highly productive joining technologies for multi-material lightweight car body structures. *Journal of Materials Engineering and Performance* 23:1515–1523.
[3] Pragana JPM, Silva CMA, Bragança IMF, Alves LM, Martins PAF (2018) A new joining by forming process to produce lap joints in metal sheets. *CIRP Annals - Manufacturing Technology* 67:301–304.
[4] Mori K-I, Bay N, Fratini L, Micari F, Tekkaya AE (2013) Joining by plastic deformation. *CIRP Annals - Manufacturing Technology* 62:673–694.
[5] Sprovieri J (2018) Advances in self-piercing riveting. *Assembly* 2:94431.
[6] Chen C, Fan S, Han X, Zhao S, Cui M, Ishida T (2017) Experimental study on the height-reduced joints to increase the cross-tensile strength. *International Journal of Advanced Manufacturing Technology* 91:2655–2662.
[7] He X (2017) Clinching for sheet materials. *Sci Technol Adv Mater* 18(1):381–405.
[8] Sampaio RFV, Larue P, Pragana JPM, Bragança IMF, Silva CMA, Martins PAF (2023) Double-flush riveting by punching and compression. *Journal of Advanced Joining Processes* 8:100155.
[9] MCG – Mind for Metal (2024) Hi-REV – Recovery of the automotive components sector. https://www.mcg.pt/research-development/hi-rev-the-future-starts-here/; 2024 Accessed in Feb, 2025.
[10] Nielsen CV, Martins PAF (2021) *Metal Forming: Formability, Simulation, and Tool Design*, 1st edition Academic PressNew York, USA.
[11] ISO 14589:2000 (2000) *Blind Rivets - Mechanical Testing*, International Organization for StandardizationGeneva, Switzerland.
[12] Jepps L, Briskham P, Sims N, Susmel L (2023) Investigation into the effect of interlock volume on SPR strength. *Materials (Basel)* 16:2747.